



220715

UCRL-JC-111789
PREPRINT

Calibration of a Wound Monitoring System Using Monte Carlo Techniques

D. P. Hickman
D. A. Kruchten
S. K. Fisher
A. L. Anderson

This paper was prepared for submittal to
Health Physics Journal

February 8, 1993



Lawrence
Livermore
National
Laboratory

This is a preprint of a paper intended for publication in a journal or proceedings. Since changes may be made before publication, this preprint is made available with the understanding that it will not be cited or reproduced without the permission of the author.

DISCLAIMER

This document was prepared as an account of work sponsored by an agency of the United States Government. Neither the United States Government nor the University of California nor any of their employees, makes any warranty, express or implied, or assumes any legal liability or responsibility for the accuracy, completeness, or usefulness of any information, apparatus, product, or process disclosed, or represents that its use would not infringe privately owned rights. Reference herein to any specific commercial products, process, or service by trade name, trademark, manufacturer, or otherwise, does not necessarily constitute or imply its endorsement recommendation, or favoring of the United States Government or the University of California. The views and opinions of authors expressed herein do not necessarily state or reflect those of the United States Government or the University of California, and shall not be used for advertising or product endorsement purposes.

Abstract

Monte Carlo techniques have been used to establish calibration factors and predict gamma spectra for well-defined measurements, and are routinely used to predict shielding requirements and criticality specifications. The Lawrence Livermore National Laboratory is researching the feasibility of using Monte Carlo techniques to establish calibration factors for *in vivo* measurement systems. A pilot study was conducted to demonstrate the use of the Monte Carlo technique to calibrate *in vivo* measurement systems, to predict the efficiency of a wound measurement system and compare the predicted efficiency with the measured efficiency, and to investigate the effects of the source geometry and the detector size on the measured efficiency. Results of this study demonstrate good agreement between the Monte-Carlo-predicted efficiency and the measured efficiency for a wound calibration phantom. The effects of the source geometry and the detector size tend to conform to the physical processes that govern the measurement process. These results demonstrate that the Monte Carlo technique accurately predicts the *in vivo* measurement efficiency if the characteristics of the attenuating material and the Monte Carlo source geometry are properly established.

Introduction

The *in vivo* measurement of radionuclides in the body usually provides confirmation of workplace controls; however, occasional measurement of internally deposited radionuclides is required to evaluate intake. The *in vivo* measurement of a wound after injury is important for initially estimating the internal dose. Over the long term, the accuracy of measuring radionuclides within a wound is important because the rate of loss of body fluids from the wound requires careful assessment relative to excretion pathways to ensure mass balance and to perform a final dose determination.

Measurement of small wounds can be performed using various detectors, such as the NaI(Tl), CdTe, and hyper-pure germanium. However, measurement of low-energy photon emitters within wounds usually requires a detector that has minimal background and high efficiency for the photon energies of interest (e.g., a thin NaI crystal). Usually, the detector sizes are small in diameter (25 mm or less) and are sometimes collimated or have an extremely small sensitive volume so that mapping of the wound can be performed.

Regardless of the size and style, accurate calibration of a detector to measure radionuclides within a wound is dependent on the calibration standard used and the degree to which the measurement of the standard conforms to the geometry associated with the measurement of the wound. For very low photon energies (e.g., 17 keV), the degree of attenuation caused by overlying tissue and tissue composition is also important. The geometry of the wound comprises two basic components: the source geometry (i.e., how the source is distributed within the wound) and the solid angle of photon emissions from the source subtended by the detector.

These basic principles of measurement are used to calibrate *in vivo* measurement systems. Measurement of internally deposited radionuclides usually requires the use of surrogate human structures (i.e., phantoms) that reasonably emulate the human subject or parts of the human subject (e.g., a hand or finger). Often times the source geometry and the amount of

overlying tissue and tissue composition are unknown. However, several techniques, such as using large surface-area detectors located at a near distance to the source or moving the source far away from the detector so that it can emulate a point source, tend to alleviate the problems associated with unknown source geometry. Even though these techniques are useful, they have technical trade-offs that may not meet the needs of the *in vivo* measurement facility.

The two purposes of the experimental study described in this paper are (1) to demonstrate that the efficiency of an *in vivo* measurement system can be predicted using standard physical principles and Monte Carlo simulation; and (2) to assess the degree of error associated with the detector efficiency if the phantom for a defined measurement system does not adequately emulate alternate source distributions within the wound.

Methods

Wound Phantom and Measurement System Description

The system used to measure small wounds at LLNL consists of a 25.4-mm diameter, 1.6-mm-thick sodium iodide crystal (NaI) mounted in a specially designed positioning platform. The face of the detector is covered with a 0.2-mm-thick Be window. Traditionally, this system has been calibrated using a simple phantom arrangement of tissue substitutes layered within an acrylic holding block. Three different types of tissue substitutes, 100% muscle, 70% muscle/30% adipose, and 50% muscle/50% adipose, are used to establish efficiency curves as a function of tissue depth and tissue composition. These polyurethane-based tissue simulants were developed at LLNL and have been described by Griffith (1980). The experiment described in this paper used 100% muscle simulant, the density and material composition of which can be found in *ICRU Publication #44, "Tissue Substitutes in Radiation Dosimetry and Measurement"* (ICRU 1989).

Square slices of muscle simulant 38 mm × 38 mm, ranging from 5 to 11 mm in thickness, were stacked within the acrylic holding block to simulate the

tissue thicknesses covering a point-source wound. The block was originally constructed to allow for calibration of the wound monitoring system for source depths to 30 mm within the tissue. However, it was extended for this experiment to allow for efficiency calibration up to depths of 68 mm (see Figs. 1 and 2).

Development of a Monte Carlo Input File

The input file that successfully emulates the measurement system within a Monte Carlo simulation requires an accurate description of the measurement geometry and the attenuating materials. For this experiment, the Monte Carlo Neutron Photon (MCNP) code was used to perform the Monte Carlo computations (Radiation Shielding Information Center 1991). The geometry input for the LLNL wound phantom and the measurement system was generated using SABRINA, a three-dimensional geometry-modeling program for MCNP (West 1986). The geometry and surface output from SABRINA were directly incorporated into the MCNP input file, and the source description and its geometry were entered using a text editor. The source used for the Monte Carlo simulations consisted of a point source that emitted 60-keV photons, thereby emulating ^{241}Am photon emissions.

Attenuating materials were described by providing the MCNP input file with the density and elemental composition of the materials. The principal materials within the MCNP input file were acrylic, LLNL muscle simulant, air, Be, and NaI(Tl). The steel casing surrounding the sides of the detector was not modeled because the coherent-scattering cross section for the 60-keV photon that originated from a point source was too small to allow full-energy scatter into the side of the detector.

The muscle simulant was modeled as a single rectangular block of material (26 mm \times 38 mm \times 70 mm) within the cavity of the acrylic holding block. This model allowed for simple movement of the point source through the tissue by editing a single line within the MCNP input file. The depths of the

point source emulated those of the overlying tissue used in the wound phantom measurements (see Table 1).

Wound Phantom Measurements

A National Institute of Standards and Technology (NIST) traceable ^{241}Am point source with a source strength of 1.3×10^4 photons per second was used to establish the measured efficiency as a function of tissue depth. The point source was initially measured on the surface of the phantom; subsequent measurements were performed, burying the point source deeper and deeper beneath layers of muscle simulant slices. For each measurement, the point source was manually positioned along the centerline of the detector in-between slices of muscle-equivalent material. Although the position of the source was constant relative to the centerline of the detector, the geometry of the measurement changed with each subsequent burial because the distance of the source from the detector also changed with each measurement. This geometry effect is often referred to as "inverse square," and is a major impetus for generating *in vivo* calibration curves as a function of overlying tissue depth.

Spectral data were collected on a multichannel analyzer with a peak region of interest extending from 50 to 65 keV. Measurements were performed for a count period of 600 seconds; the efficiency was calculated using the following:

$$\% \text{efficiency} = \frac{\text{CPS}_{\text{Gross}} - \text{CPS}_{\text{Background}}}{\text{gammas / s}} \times 100$$

Evaluation of Alternate Source and Detector Geometry

When a worker has a wound, it is unlikely that the radioactive material will completely reside within the wound as a point source. It is reasonable to assume, however, that some of the radioactive material will be distributed

along the puncture or cutting edge of the wound. In an effort to study the effect on the efficiency because of varying source distribution, a Monte Carlo simulation was used to predict the efficiency for an alternate source geometry. This geometry consisted of a line source perpendicular to the surface of the detector, penetrating the phantom to depths between 5 and 30 mm.

Because many different styles of detectors are used to measure wounds, the effect of using an alternate detector was also studied. The 25-mm detector was replaced with a square 152 mm NaI(Tl) detector; both were modeled as 1.6-mm-thick detectors. Tallies were generated for the point source and the perpendicular line-source geometry at depths between 5 and 30 mm.

Results

Results from the Monte Carlo method were expected to be accurate and consistent with the measured values within a constant adjustment factor. This factor was determined by dividing the measured efficiency when the point source is resting on the surface of the phantom (i.e., 0 mm depth) by the MCNP-predicted response (i.e., tally) for a point source that is centered under the detector and rests on the surface of the phantom. MCNP output results at depths below the phantom surface were multiplied by the adjustment factor to predict the absolute efficiency. The adjustment factor changes the intercept of the MCNP-predicted calibration curve but maintains the shape of the curve as a function of depth. Therefore, it is reasonable to conclude that the Monte Carlo technique is successful when the appropriate correction factors are generated and if the shape of the MCNP-predicted efficiency curve is equal to the shape of the measured efficiency curve. Table 1 provides the measured and predicted efficiencies obtained from this study. Figure 3 provides a visual representation of the data that can be used to evaluate the shapes of the efficiency curves as a function of depth.

Monte-Carlo-predicted efficiencies for wound depths less than 57 mm were within 12.5% or less of the measured efficiency for the LLNL wound phantom. Depths of 63 and 68 mm demonstrated the most difference from

the measured values—25% and 32%, respectively. The observed differences are of little concern when measuring wounds, and may be attributed to factors such as less reliability in measurements at extreme depths and uncertainties in elemental contents of the muscle substitute material.

Table 2 compares a point source to a line source in the wound phantom. The difference in the calibration factor for a line source, as opposed to that for a point source, is less than 13% for wound penetrations that are less than 5 mm deep. For penetrations greater than 10 mm, the differences are more significant—ranging from 50 to 277%, respectively, for penetrations between 10 and 30 mm. At all depths, the absolute efficiency for the point source is less than that for the line source. This result implies that conservative estimates (i.e., overestimates) of activity in the wound will occur if the source is distributed and a point source is used to calibrate the wound measurement system.

The relative efficiencies for measuring a point source and a line source using a square 152-mm \times 1.6-mm-thick NaI(Tl) detector are provided in Table 3. The difference in depth between a point source and line source is smaller using the square 152-mm detector, as opposed to using the 25.4-mm diameter detector. The ratio of the line-source efficiency to the point-source efficiency to depths of 30 mm was less than 50% with the square 152-mm detector. In contrast, a 50% difference in efficiency was observed for the line source and the point source within 10 mm of penetration using a 25.4-mm diameter detector.

Conclusions

The agreement is good between the measured and predicted efficiencies for a point source to depths of approximately 60 mm. Between depths of 0 and 57 mm, the Monte-Carlo-predicted efficiency and the measured efficiency agreed to within 12.5%. The Monte Carlo efficiency tended to slightly underestimate the efficiency and provide a conservative estimate (i.e., overestimate) of activity in the wound. The differences between the

measured and Monte-Carlo-predicted efficiencies at depths of 63 and 68 mm may be caused by the density and material specifications used in the Monte Carlo code, because the solid angle effects decreased with increased source distance.

Significant differences can occur in the efficiency because of the source geometry (Fig. 4). If a point source is used to calibrate a measurement system that is subsequently used to measure a wound in which the source distribution is significantly different from a point source (e.g., a line source), then the calibration of the point source tends to provide conservative estimates (i.e., overestimates) for activity in the wound. The differences in efficiency appear to be more significant for penetrations greater than 5 mm, especially if the calibration was made using a 25.4-mm diameter detector.

The errors associated with an unknown source geometry (e.g., a point source versus a line source) can be minimized using a large surface-area detector (Fig. 4). This is evident from the Monte Carlo computations and from a basic understanding of the physical processes involved in the measurement. Detectors with small surface areas subtend smaller solid angles. As the source penetrates deeper into the wound or as the source geometry changes, the effects of the smaller solid angle subtended by the smaller detector become more pronounced. At greater distances from the detector, the effects of solid angle changes become minimal and the effects of attenuation by intervening materials become dominant. These effects can be observed in Fig. 1, where the efficiency for measuring a point source has a two-component appearance. The rapid component of the efficiency curve at shallow depths is due largely to geometry effects. At greater depths, the other component is less dominated by the geometry effects and more dominated by attenuation effects. A similar effect can occur by moving a line source away from the detector. At greater distances from the detector (relative to the diameter of the detector), however, the line source will eventually have about the same efficiency as a point source.

The conclusions reached from this study can be summarized for application as follows:

- If the *in vivo* measurement is to accurately quantify the amount of activity in the wound, then a large surface-area detector should be used because it will minimize the effects associated with an unknown source geometry.
- If the *in vivo* measurement is to characterize the wound and to direct surgical removal of the contaminant, a small detector is more appropriate. It is important to note, however, that the capability of a small detector to assess the amount of contaminant within the wound is at best semi-quantitative and can result in significant errors.

Acknowledgments

Work performed under the auspices of the Nuclear Regulatory Commission under Contract L-1952 and the U.S. Department of Energy under Contract W-7405-Eng-48 by the Lawrence Livermore National Laboratory. The authors wish to thank Dr. John Clark, Ms. Charleen Radditz, and Mr. Robert Loesch for their review of this manuscript.

Appendix A MCNP Input File

wound calibration simulation using MCNP

```

1 1 -1.19000 1 -2 3 -4 5 -6 :-7 8 3 -9 6 -10 :-2 7 3
      -4 6 -10 :-8 1 3 -4 6 -10
2 2 -1.12000 8 -7 9 -4 6 -10
3 3 -0.00129 10 -11 -12
4 4 -1.80000 11 -13 -12
5 5 -3.66700 13 -14 -12
7 0      (-1 :2 :-3 :4 :-5 :6 ) (7 :-8 :-3 :9 :-6
      :10 ) (2 :-7 :-3 :4 :-6 :10 ) (8 :-1 :-3
      :4 :-6 :10 ) (-8 :7 :-9 :4 :-6 :10 ) (-10
      :11 :12 ) (-11 :13 :12 ) (-13 :14 :12 )

```

```

$ Acrylic Jig
$ Muscle Simulant
$ Air Gap
$ Be Window
$ NaI Detector

```

```

1 px      -3.80000e+00
2 px       3.80000e+00
3 py      -2.86000e+00
4 py       2.86000e+00
5 pz       0.00000e+00
6 pz       6.75000e-01
7 px       1.90000e+00
8 px      -1.90000e+00
9 py      -9.60000e-01
10 pz      7.54100e+00
11 pz      8.14100e+00
12 c/z     0.00000e+00      7.50000e-01      1.27000e+00
13 pz      8.16100e+00
14 pz      8.32000e+00

```

```

mode p      $calculates photon transport only
c      importance card - first five cells = 1 last cell =0
imp:p 1 4r 0
c      source specification cards - point source - 68 mm depth
sdef erg=0.06 pos= 0.0 0.75 0.7284
c      tally specifications
f8:p 5
f1:p 13
e0 051 .052 .053 .054 .055 .056 .057 .058 .059 .060
c      material specifications
m1 1000 0.417 6000 0.333 8000 0.167 17000 0.083
m2 1000 -0.09 6000 -0.602 7000 -0.028 8000 -0.266 20000 -0.014
m3 7000 -0.7809 8000 -0.2095 18000 -0.0096
m4 4000 -1.000
m5 11000 -0.1534 53000 -0.8466
c      cut calculations at 50 keV
cut:p j 0.050
c      end calculations at 100,000 photons
nps 100000

```

References

Griffith, R. V. Polyurethane as a base for a family of tissue equivalent materials. Book of Papers, 5th International Congress of the International Radiation Protection Association, Vol. II, p.165. Oxford: Pergamon Press; 1980.

International Commission on Radiation Units and Measurements. Tissue substitutes in radiation dosimetry and measurement. Bethesda, MD: ICRU; ICRU Report 44; 1989.

Radiation Shielding Information Center (RSIC). MCNP 4 Monte Carlo Neutron and Photon Transport Code System. Oak Ridge National Laboratory; RSIC Report Number CCC-200A/B; 1991.

West, J. T. SABRINA: an interactive three-dimensional geometry-modeling program for MCNP. Los Alamos National Laboratory; LA-10688-M; 1986.

Table 1. Measured and Monte-Carlo-predicted efficiencies as a function of depth for a ^{241}Am point source using the LLNL wound phantom.

Table 2. Measured and Monte Carlo efficiencies as a function of penetration for a ^{241}Am point source and a perpendicular line source using the LLNL wound phantom.

Table 3. Relative Monte Carlo efficiencies as a function of penetration for a 60-keV point source and a perpendicular line source using a square 152-mm NaI(Tl) detector and the LLNL wound phantom.¹

Footnote for Table 1

* Monte Carlo pulse-height tally was multiplied by a constant adjustment factor of 53.9..

Footnote for Table 3

* Efficiencies were tallied for 50- to 60-keV regions of interest and represent the values obtained from the Monte Carlo simulations.

Table 1

Depth (mm)	Measured Efficiency (%)	Monte Carlo Efficiency* (%)
0	15.52	15.52
5	8.81	9.08
10	5.52	5.46
15	3.53	3.47
20	2.43	2.34
25	1.65	1.63
30	1.21	1.15
35	0.91	0.87
38	0.82	0.73
41	0.69	0.62
43	0.63	0.57
46	0.59	0.48
53	0.39	0.34
57	0.32	0.28
63	0.28	0.21
68	0.25	0.17

Table 2

Penetration (mm)	Line-source efficiency (%)	Point-source efficiency (%)	Ratio
0	15.52	15.52	1.00
5	10.25	9.08	1.13
10	8.18	5.46	1.50
15	6.77	3.47	1.95
20	5.76	2.34	2.46
25	4.97	1.63	3.05
30	4.34	1.15	3.77

Table 3

Penetration (mm)	Line-source efficiency (%)	Point-source efficiency* (%)	Ratio
0	50.73	50.73	1.00
5	46.23	42.46	1.09
10	43.01	36.86	1.17
15	40.47	32.59	1.24
20	38.18	29.09	1.31
25	36.18	26.12	1.39
30	34.40	23.49	1.46

Fig. 1. Acrylic holding block.

Fig. 2. Detector, positioning platform, and wound phantom used for the calibration of the wound measurement system.

Fig. 3. Measured and Monte-Carlo-predicted efficiencies as a function of depth for a ^{241}Am point source using the LLNL wound phantom.

Fig. 4. Ratio of line-source efficiency to point-source efficiency as a function of penetration depth.

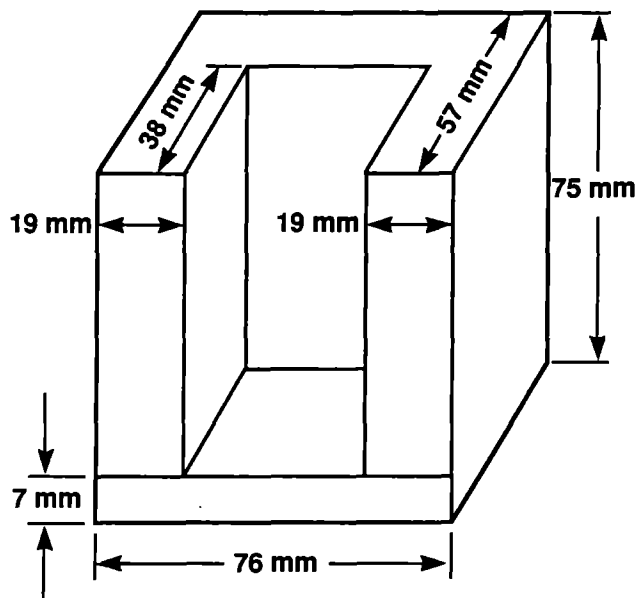
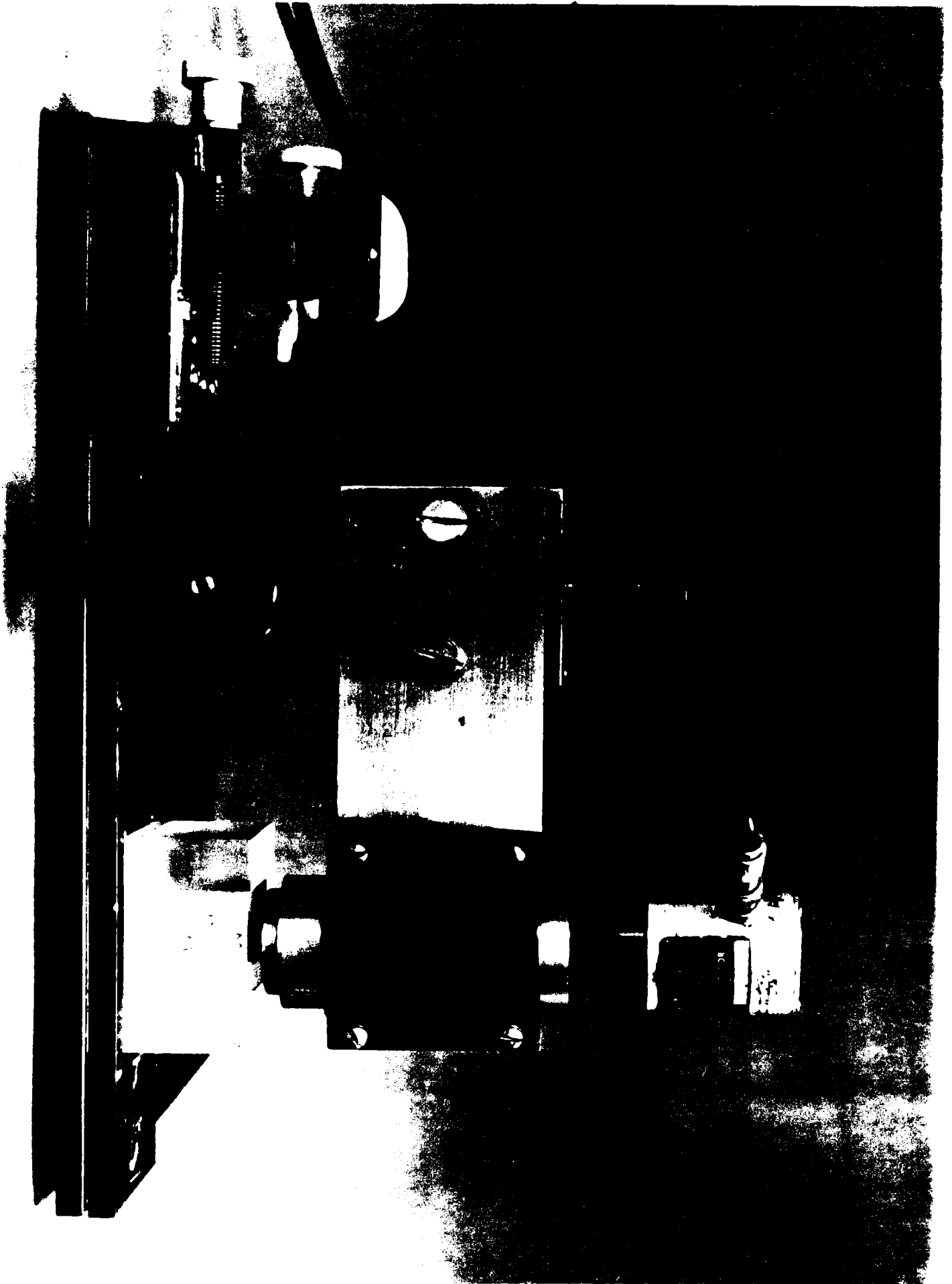


Fig 2



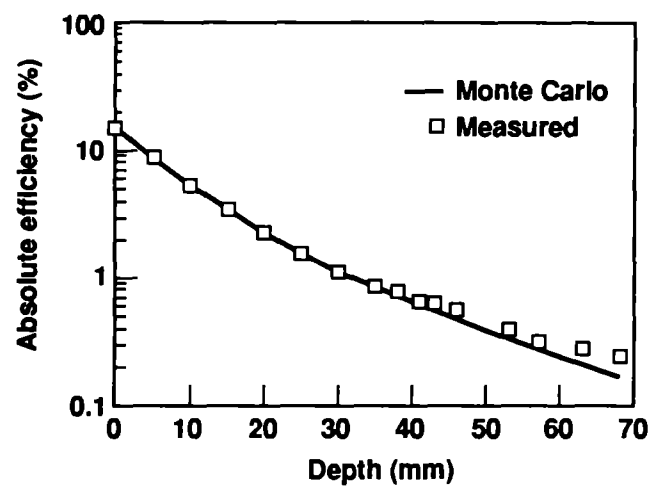


Fig. 3

